Environmental Health Perspectives
Vol. 16, pp. 161-175, 1976

Electron Spin Resonance (ESR) Study of Cigarette Smoke by Use of Spin Trapping Techniques

by William A. Pryor,*† Ken-ichi Terauchi,* and William H. Davis, Jr.*

The technique of spin trapping has been applied to the gas phase of cigarette smoke to identify and quantify the radicals present. It was found that radicals could be trapped only if the smoke was filtered. Three spin traps were used: *N-tert*-butyl-α-phenyl nitrone (PBN), 5,5-dimethyl-Δ¹-pyrroline-1-oxide (DMPO) and α-(3,5-di-*tert*-butyl-4-hydroxyphenyl)-*N-tert*-butyl nitrone (OHPBN). From the electron spin resonance (ESR) splitting constants of the radicals produced by the reaction of smoke radicals with the spin traps and also from the effect of varying the path length between the cigarette and the spin trap solution, it is concluded that three types of signals are observed. Type I signals indicate the presence of oxygenated radicals which appear to be a mixture of alkoxy radicals ($RO\cdot$) and aroyloxy ($ArCO_2\cdot$) radicals. Our data do not allow conclusions about the nature of the R or Ar groups in these two oxy radicals; however, considerations based on lifetimes suggest that the R group probably is tertiary. Type II and III signals are not typical spectra of spin adducts. Instead, we believe they result from reaction of smoke (and probably radicals in smoke) with the PBN spin trap and indicate that smoke has the ability to effect one-electron oxidations. Only type I signals are observed with DMPO and OHPBN. A quantitative study shows that 4×10^{14} spins/puff are present in the smoke, in contrast with the result of a recent study which used a very different method for determining the radical content of smoke.

A discussion of the nature of the radicals in smoke and some tentative conclusions are presented.

Introduction

It is widely recognized that cigarette smoke is pernicious and highly noxious (*1*) but, partly because smoke consists of many compounds (probably over 10,000), the mechanisms by which it produces the observed pulmonary pathology are not clear (*2,3*). However, several lines of evidence suggest that free radicals may be involved. First, it is known that radicals are present in unsmoked tobacco, in burnt tobacco, and in smoke (*4*). Secondly, there is inferential evidence linking cancer, one of the observed pathological results of continuous exposure to smoke, with free radicals (*5-10*). And, finally, there is some evidence that thiols, known to be free-radical scavengers, protect cells against the effects of smoke (*11*). For these reasons, and as part of a general study of the molecular mechanisms underlying the pathology caused by free radicals and free-radical-producing reagents, we have begun a study of the radical chemistry of cigarettes and cigarette smoke.

As our first approach to this complex problem, we have elected to utilize the technique of spin trapping to identify the radicals present in smoke. We here report initial results of that study.

*Department of Chemistry, Louisiana State University, Baton Rouge, Louisiana 70803.

†Author to whom correspondence and requests for reprints should be addressed.

Lyons et al. (*12*) first detected ESR signals from free radicals in tobacco smoke condensate which was trapped at liquid oxygen temperatures. In subsequent years, several ESR studies have been reported on whole cigarette smoke condensates at low temperatures (*13-16*). The interaction of smoke radicals in whole main stream smoke with blood or tissue also has been demonstrated by ESR (*9*). However, less attention has been paid to the radical chemistry of the gas phase of smoke, although it is known that the gas phase is, under some experimental conditions at least, as toxic as the condensed phase (*14,17,18*). It appeared likely to us that the recently developed techniques utilizing spin traps could be applied to identify and quantify the radicals present in the gas phase of smoke.

The spin trapping method for identifying radicals is based on the reaction (*19-21*) shown in eq. (1).

$$\underset{\text{(paramagnetic)}}{\text{short-lived radical}} + \underset{\text{(diamagnetic)}}{\text{spin trap}} \longrightarrow \underset{\text{(paramagnetic)}}{\text{spin adduct}} \quad (1)$$

Thus, the short-lived radicals in gas-phase smoke combine with the spin trap reagent to give relatively stable free radicals (spin adducts) which can be detected by ESR. From the values of the nuclear hyperfine splitting constants of spin adducts, it is possible to evaluate the character of short-lived radicals in the system. In this communication, we wish to report the results obtained from the ESR study of the reaction of filtered but unfractionated gas phase smoke radicals with several spin traps at room temperature. The spin traps we have used are *N-tert*-butyl-*α*-phenyl nitrone (PBN), 5,5-dimethyl-Δ¹-pyrroline 1-oxide (DMPO), and *α*-(3,5-di-*tert*-butyl-4-hydroxyphenyl)-N-*tert*-butyl nitrone (OHPBN).

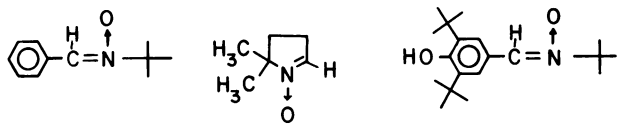

PBN DMPO OHPBN

Experimental

Materials

Three spin trap reagents were used in this study. *N-tert*-butyl-*α*-phenyl nitrone (PBN) was obtained from Eastman Kodak Co. (Rochester, N.Y.) and used without further purification. 5,5-Dimethyl-Δ¹-pyrroline-1-oxide (DMPO) was prepared by reduction of 2-(3-methyl-3-nitrobutyl)-1, 3-dioxolane (*22*). Our material has bp 78°C/1.2 mm (lit. bp 66-67°C/0.6 mm). *α*-(3,5-Di-*tert*-butyl-4-hydroxyphenyl)-*N-tert*-butyl nitrone (OHPBN) was prepared from 3,5-di-*tert*-butyl-4-hydroxybenzaldehyde and *tert*-butylhydroxylamine (*23*) and purified by recrystallization from ethanol. It melts above 200°C with decomposition. It has NMR peaks (in $CDCl_3$) at *δ*: 1.48 (*s*, 18H), 1.64 (*s*, 9H), 5.52 (*s*, 1H), 7.42 (*s*, 1H), 8.20(*s*, 2H). Benzene, used as a solvent in spin trap solutions, was purified by the ordinary method and stored over 3Å molecular sieves. Nitric oxide and nitrogen dioxide gases were obtained from Matheson. The cigarettes used in this study were research cigarettes, grade R kindly supplied by the University of Kentucky Tobacco and Health Research Institute, and nonfiltered commercial cigarettes. Grade R research cigarettes were used unless otherwise noted.

Smoking Conditions

The cigarettes were smoked under the following standard conditions which are meant to approximate the average puffing pattern of humans (*2*): one 35-ml puff of about 2 sec duration every 20 sec. An average of 20 puffs per cigarette was obtained. The manual smoking machine employed in this study consists of a syringe connected through a silica gel tube and a valve to a glass capillary for passing the smoke into the spin trap solution (Fig. 1.) The glass capillary (20 cm long, ca. 0.6 mm o.d.) was connected to a Cambridge filter holder leading to a small tube containing 4 ml of the spin trap solution. The total path length between the cigarette and the spin trap solution is 37 ± 0.5 cm. This, therefore, is the minimum path length we could study. Experiments in which the path length was varied were conducted

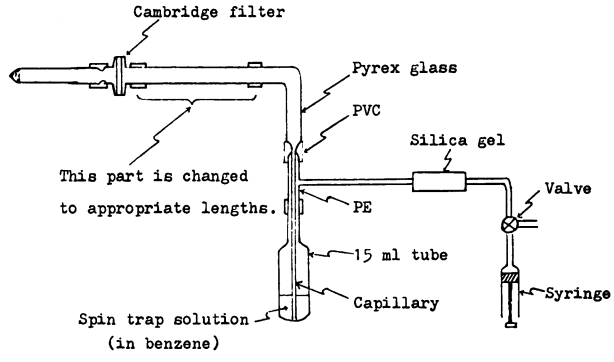

FIGURE 1. A diagram of the manual smoking apparatus used.

by using a Pyrex tube (7.4 mm i.d.) of appropriate length to change the distance between the Cambridge filter (4.5 cm in diameter) and the glass capillary. The distances given below as the smoking path lengths are the lengths of the variable section of Pyrex tubing; therefore, when the length is given as 20 cm long, the actual smoking path length including the capillary is ca. 57 cm. Since the filter was observed to fracture after more than six cigarettes, it was changed after four cigarettes had been smoked. In the experiments using filter paper, a filter paper holder of 6.9 cm i.d. was used. The measurements of the weight of condensed materials were made under the same conditions as used in the smoking path length study but with only benzene in the trap. The benzene was allowed to evaporate from the brown-colored solutions, and the residue was weighed.

Preparation of Particulate Matter Solution

The particulate matter (PM) solutions in this study were prepared as follows. After four cigarettes were smoked under the conditions described above, the Cambridge filter was placed in a shell extraction paper (80 × 25 mm) and extracted by refluxing with 100 ml benzene for 4 hr. The resultant brown-colored benzene solution was condensed to less than 20 ml by using nitrogen gas flow at room temperature and then diluted with benzene to 25 ml to yield a solution containing 159.1 mg PM per 25 ml benzene. This concentrated PM solution was further diluted to give PM concentrations in the range 2.5-12.5 mg/10 ml that was observed in the smoking experiments. These solutions of lower PM concentrations were then used to investigate the effect of added PM on the rate of decay of the spin adduct signals.

Spin Trapping Method

The PBN was dried in a vacuum desiccator because of its hygroscopic character. The DMPO and OHPBN were purified by vacuum distillation and recrystallization, respectively, immediately before use. The concentration of spin trap solution used was 0.05*M* in purified benzene. No ESR signal was observed from the spin trap solutions before they were exposed to smoke.

ESR Measurements

ESR spectra were measured with a JEOL Model JES-3BS X-band spectrometer operating at about 9.4 GHz using 100 Kc field modulation. The frequency was monitored with a calibrated absorption wavemeter incorporated in the microwave unit. Field sweep calibration was checked with stable diphenylmethyl-*tert*-butyl nitroxide radical in benzene (*24-26*). The nuclear hyperfine splitting constants (hfsc) were obtained by averaging the spacings between peaks as well as between crossover baseline points. The *g*-factors were calculated by using 2,2-diphenyl-1-picrylhydrazyl (DPPH) free radical as a standard (g=2.0036). Quartz sample tubes were employed. Deoxygenation was achieved by bubbling helium gas through the solution in the ESR tube using a glass capillary. A calibration curve obtained from a series of concentrations of purified DPPH in benzene was used to determine the smoke radical concentration.

Computer Simulation

A computer was used to produce simulations of the complex spectra that result when several smoke radical-spin adducts are present in a solution. The program was kindly supplied by Dr. Brian J. Hales of this Department. The parameters used for computer simulation were experimentally measured, and typical values are summarized in Table 1.

Table I. Parameters observed for the spin adducts of oxy radicals with PBN and DMPO and used in computer simulations of ESR spectra.

Spin adducts [a]	hfsc, gauss		Line width
	a^N	a_β^H	ΔH_{pp}, gauss [b]
BzO-PBN	13.25	1.49	0.532
t-BuO-PBN	14.18	1.93	0.940
Ph-PBN	14.45	2.15	0.925
BzO-DMPO	12.19	10.15	1.716
t-BuO-DMPO	13.05	7.52 [c]	1.394
Ph-DMPO	13.96	19.47	0.926

[a] BzO is $PhCO_2$ and *t*-BuO is *t*-C_4H_9O.
[b] Peak-to-peak line width.
[c] Also a_γ^H= 2.04 gauss.

Results

Since the ESR results to be discussed are complex, it will be helpful to the reader to summarize some of our conclusions at this point so the identification of the signals can be given as the data are discussed. In brief, we find three types of ESR signals. Type I appears to be due to a mixture of the spin adducts of two types of oxy

radicals, alkoxy (RO·) and aroyloxy ($ArCO_2$·). Type II and III signals are not typical spectra of spin adducts. Instead, we believe they result from reactions of smoke, and probably radicals in smoke, with the PBN spin trap and indicate that smoke has the power to perform one-electron oxidations. Signals of all three types are observed with PBN, but only a type I signal is observed with DMPO and with OHPBN.

PBN Spin Trap

Figure 2 shows a typical spectrum observed from the spin adduct produced when PBN is exposed to smoke from nine cigarettes that had been passed through a Cambridge filter. The spectrum consists of two signals which are superimposed: a typical PBN-spin adduct (type I signal), in which the nitrogen triplet is split into doublets giving a six-line spectrum; and a broad triplet signal with 1:1:1 relative intensities (type II), suggestive of a second nitrogen hyperfine interaction and assigned $a^N \cong 10$ gauss. (Type III signals, which are not observed at this short path length, will be described below.) A similar spectrum was obtained from commercial cigarettes (nonfilter tip), with the smoke filtered either through a Cambridge filter or a piece of filter paper (Fig. 3). The hyperfine splitting constants (hfsc) obtained from a series of experiments like

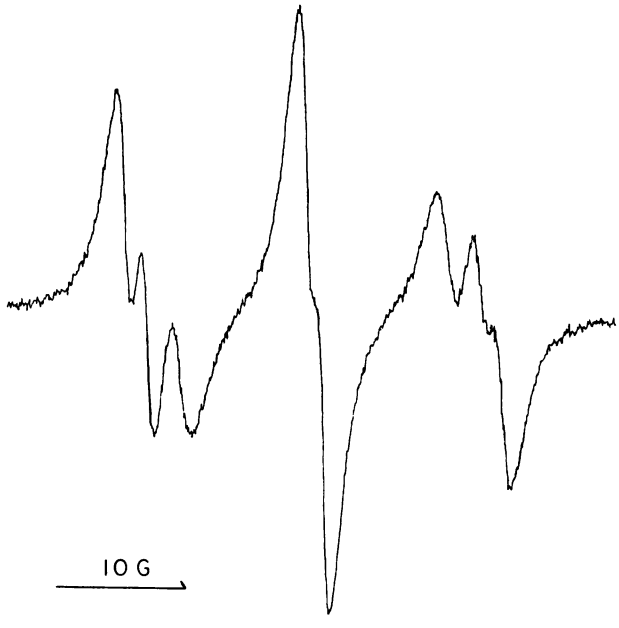

FIGURE 2. Typical ESR spectrum of smoke radicals-PBN spin adducts at room temperature in benzene. R grade cigarettes and Cambridge filters were used.

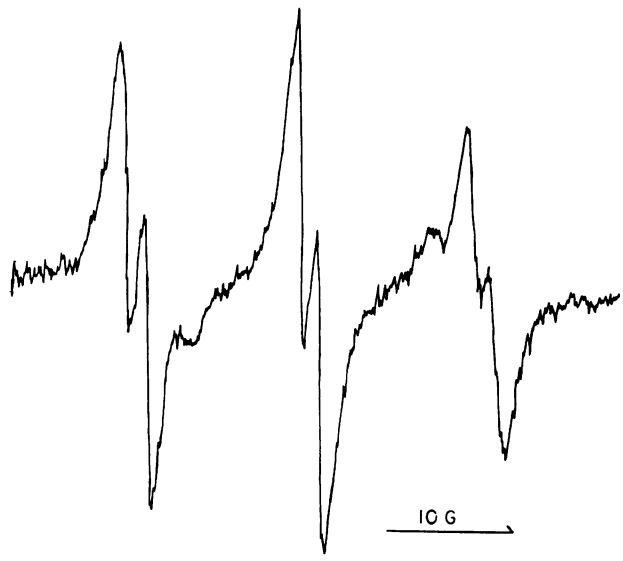

FIGURE 3. Typical ESR spectrum of smoke radicals-PBN spin adducts from the nonfiltered commercial cigarettes and filter paper experiment.

those represented by Figures 2 and 3 are summarized in Table 2. If no filter was used, no signals could be detected. A possible explanation for this is given below.

A significant change in the ratio of the type I and type II signal intensities occurred after the solutions had been allowed to stand for 1 hr. The six-line signal showed a rapid decay compared to that of the broad triplet. The values of the hfsc do not appear to change with time. The reproducibility of the data in this study is indicated by the values for duplicate runs given in Table 2. The data of Bluhm et al. (*27*) and Wasson et al. (*28*), who used a PBN spin trap system under different conditions from the present study, are also listed in Table 2 to facilitate comparisons. These results will be discussed later.

Most of the spin adducts of PBN have similar values of nuclear hfsc. Thus, the use of other spin traps is necessary to identify the nature of the radicals trapped. For this reason, we next studied DMPO, which gives spin adducts with β-hydrogen hfsc values that are more sensitive to the structure of the radicals trapped than are those of PBN (*29*).

DMPO Spin Trap

The ESR spectrum obtained from the DMPO spin adduct of gas phase smoke radicals, again filtered through a Cambridge filter, consists of six broad lines, with hfsc estimated to be $a^N = 13.0$

Table 2. Results of spin trapping studies of cigarette smoke by using PBN.[a]

System and run no.[b]	Number of cigarettes	Concn of PBN, M[c]	Type I signal, gauss[1]		Type II signal
			a^N	a_β^H	a, gauss
R1	5	0.05	13.9±0.2[d]	2.08	10.0
R2	6	0.05	13.9±0.3	2.0±0.2	10.2
R5	9	0.05	13.9±0.5	1.8±0.5	10.2
C12	8	0.05	13.9±0.2	1.9±0.3	10.8
Bluhm et al.	e	0.05	13.8±0.1	1.99±0.10	n.d.[f]
Wasson et al.	3[g]	0.2	15.0	n.d.[f]	n.d.[f]

[a] All measured at room temperature.
[b] R and C indicate "R" grade research or commercial cigarettes, respectively.
[c] Benzene was used as solvent.
[d] Mean ± S.D.
[e] Five 20 ml puffs: see Bluhm et al. (*27*).
[f] Not detected.
[g] See de Hys et al. (*28*).

± 0.2 and a_β^H=10.1 ± 0.3 gauss. A representative spectrum is illustrated in Figure 4.

Compared to the PBN system signals, the ESR signals in Figure 4 show a more rapid decay with time. In addition, during the first half hour after the initial measurements, they are significantly altered to a different spectrum with a^N=13.7 and a_β^H=11.3 gauss. These observations suggest that at least two types of signals are being observed, and this finding appears to be consistent with the change in the relative intensities of the two signals observed in the PBN system with time. The hfsc values for the initially observed DMPO spin adduct are summarized in Table 3, together with some ESR data of known organic radicals.

OHPBN Spin Trap

Some studies were performed with the use of OHPBN as the spin trap, since it has been reported to yield different ESR signals for carbon-centered and oxygen-centered radicals. Pacifici and Browning (*30*) found that OHPBN reacts with oxy radicals at its OH group [eq. (2a)], whereas carbon radicals add to the nitrone function [eq. (2b)].

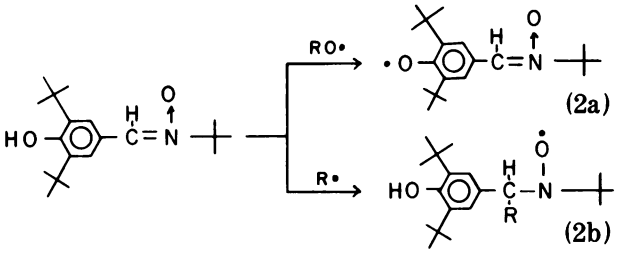

The observed ESR spectrum of smoke radical-spin adducts from 0.05M OHPBN in benzene solution has a^N=5.0, a_b^H=2.8, a_m^H=1.7 and 1.5 gauss (two nonequivalent aromatic protons). As is clear from Table 4, the observed hfsc values from cigarette smoke indicate a fair agreement with those of phenoxy radicals, suggesting the presence of oxygen-centered radicals in the smoke. Furthermore, the formation of nitroxide radicals from addition of carbon-centered radicals to the nitrone is not observed, suggesting the absence of carbon-centered radicals which are stable enough to survive the passage through the glass tubing and the Cambridge filter arrangement of our experiments.

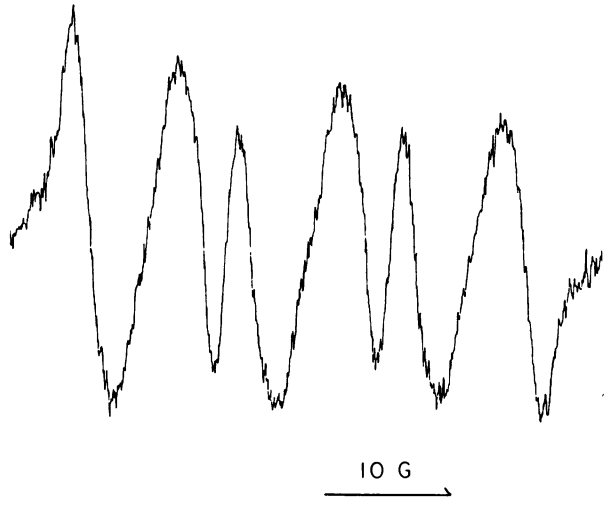

FIGURE 4. ESR spectrum of cigarette smoke radicals-DMPO spin adducts at room temperature in benzene.

Effect of Smoking Path Length

A study of the effect of smoking path length was made in an effort to provide information about the lifetime of the radicals in smoke. It was hoped that short-lived radicals in the smoke might undergo a rapid decay and allow observation of longer-lived, more stable radicals. To our surprise, the longer path length experiments were found to give cleaner ESR signals, suggesting a higher concentration of smoke radicals.

Table 3. Results of spin trapping studies of cigarette smoke and known radicals with DMPO.

Radical source	Number of cigarettes	Concn. of DMPO, M [a]	Nitroxide[b] a^N, gauss	a^H_β, gauss	a^H_γ, gauss
Smoke radicals					
R6	10	0.053	13.0±0.2	10.1±0.3	
R7	15	0.05	13.2±0.1	9.2±0.1	
C14	10	0.05	13.0±0.1	8.3±0.4	
Known radicals					
$CH_3\cdot$		0.05	(14.31)[c]	(20.52)	
$C_6H_5\cdot$		0.05	14.0[d]	19.4	
			(13.76)[d]	(19.22)	
t-$C_4H_9O\cdot$		0.05	13.2[e]	7.6	2.2
			13.0[f]	7.8	2.0
			(13.11)[e]	(7.93)	(1.97)
$C_6H_5CO\cdot$		0.05	(13.99)[g]	(15.57)	
$C_6H_5COO\cdot$		0.05	12.2[h]	10.2	n.d.[i]
			(12.24)[h]	(9.63)	(0.87)

[a] All measured in benzene at room temperature.
[b] Literature values are shown in parentheses; see Janzen and Liu (*29*).
[c] Photolysis of methylmercury iodide.
[d] Thermal decomposition of phenylazotriphenylmethane at 60°C.
[e] Thermal decomposition of di-*tert*-butyl peroxide at room temperature.
[f] Thermal decomposition of di-*tert*-butyl peroxide at 60°C.
[g] Hydrogen abstraction from benzaldehyde by benzophenone triplet.
[h] Thermal decomposition of benzoyl peroxide at 60°C.
[i] Not detected.

A typical ESR spectrum obtained from the experiments using a 60 cm smoking path length, and the PBN spin trap system is shown in Figure 5.

Spectra from longer path length experiments, such as that shown in Figure 5, are interpreted in Table 5 in terms of three types of signals: type I,

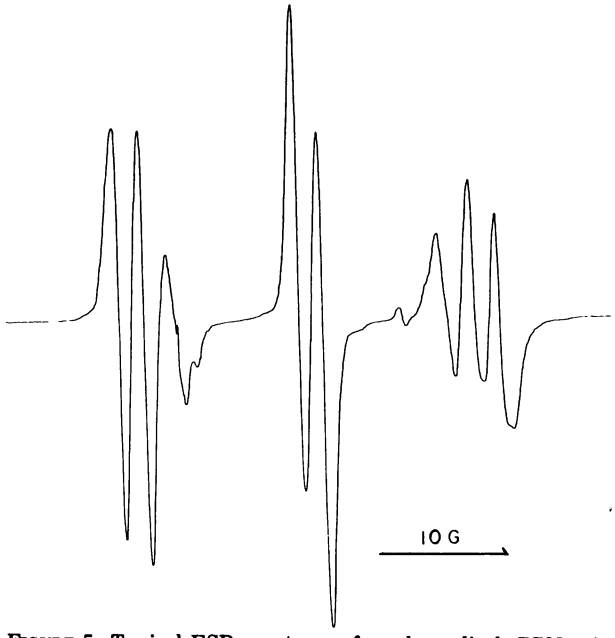

FIGURE 5. Typical ESR spectrum of smoke radicals-PBN spin adducts in benzene obtained by using a 60 cm smoking path length.

Table 4. Results of spin trapping studies of cigarette smoke and known radicals with OHPBN.[a]

Source	Number of cigarettes	a^N, gauss	a^H_β, gauss	a^H_m, gauss	
Smoke radicals					
R8	10	5.1	2.9	1.7	1.5
C13	6	4.9	2.7	1.6	1.5
Known radicals		Nitroxide			
$C_6H_5\cdot$		14.6[b]	2.3[b]		
$(CH_3)_2\dot{C}CN$		13.4[b]	3.7		
			Phenoxyl		
$C_6H_5COO\cdot$		5.05[b]	2.60	1.70	1.50[b]
$CH_3COO\cdot$		5.05[b]	2.60	1.70	1.50

[a] All measured in 0.05M OHPBN in benzene at room temperature.
[b] Literature values; see Pacifici and Browning (*30*).

a triplet of doublets with a^N=13.8 and a^H_β=1.9 gauss and with g=2.0061, appears to be due to a mixture of the PBN spin adducts of two species of oxy radicals, alkoxy (RO·) and aroyloxy (Ar-$CO_2\cdot$). The other two types of signals are a broad 1:1:1 triplet with $a^N\cong$10.4 gauss and g=2.0061 (type II), and a 1:1:1 triplet with a^N=8.1 gauss and g=2.0064 (type III). We believe the type II and III signals do not arise from normal PBN spin adducts; instead we suggest they result from the reaction of smoke, and probably radicals in smoke (see below), with PBN. We tentatively suggest that the type II signal shows a nitrogen hyperfine

Table 5. Effect of smoking path length on the results of spin trapping studies of cigarette smoke with PBN and DMPO.[a]

Path length, cm	PBN				DMPO (Type I)	
	Type I		Type II,	Type III,		
	a^N, gauss	a^H_β, gauss	a^N, gauss	a^N, gauss	a^N, gauss	a^H_β, gauss
0	13.9±0.3	1.9±0.2	10.2	n.d.[b]	13.2±0.1	9.2±0.1
20	13.9±0.1	1.8±0.1	10.1	n.d.[b]	13.3±0.6	8.9±0.1
40	13.9±0.1	1.9±0.1	10.5	7.9	13.1±0.1	8.0±0.2
60	13.8±0.1	1.9±0.1	10.6	8.1	13.1±0.1	7.9±0.3
80	13.8±0.2	1.8±0.2	10.2	8.1	—	—
100	13.8±0.1	1.9±0.1	10.4	8.1	—	—
120	13.9±0.1	1.9±0.1	10.6	8.1	13.2±0.1	8.2±0.3
180	13.8±0.1	1.8±0.2	10.4	n.d.[b]	13.8±0.6	8.8±0.4
g Factor	2.0061±0.0001		2.0061±0.0001	2.0064[d]	2.0068±0.0002	

[a] All measured in 0.05*M* nitrone in benzene at room temperature by using eight R grade cigarettes. All values mean ±standard deviation.
[b] Not detected.

splitting. We are studying the reactions of several smoke constituents (e.g., alkyl nitrites) with PBN in an effort to identify the radical(s) which produce the type II signal.

A signal that has $a^N = 7.67$ gauss and is similar to the type III signal was reported by Janzen and Blackburn (*26*) from the reaction of PBN with a variety of oxidizing agents such as chlorine, bromine, and substituted perbenzoic acids. They suggest that this spectrum is due to benzoyl-*tert*-butyl nitroxide, PhCO-N(−O·)-*t*-C_4H_9. We, therefore, tentatively infer that our type III signal is also due to this one-electron oxidation product from PBN.

In an effort to identify the type III signal, we studied the reactions of nitric oxide (NO) and nitrogen dioxide (NO_2) with PBN. It is known (*31,32*) that smoke contains a relatively high concentration of both NO and NO_2. When PBN solutions are exposed to either NO or NO_2, the same signal is observed, a triplet very much like the type III signal with $a^N = 8.0$ gauss. This is not the signal expected for the spin adducts of either NO or NO_2 with PBN, therefore, we conclude that these nitrogen oxides, both of which are free radicals, may oxidize PBN to produce a type III signal. An opposite conclusion has been reached by other workers. de Hys et al. (*28*), using a 0.2*M* PBN solution in benzene, did not observe the triplet which they found characteristic of NO_2 ($a^N \cong 10$ gauss) in their cigarette smoke spectrum. They therefore concluded (*28*) that NO_2 was not the radical present in smoke.

In contrast with PBN, the ESR spectrum obtained from the DMPO-cigarette smoke system with a 60 cm path length is more complicated, as is shown in Figure 6, than is the shorter path length spectrum shown in Figure 4. Although such a noisy spectrum is rather hard to interpret, it is clear from Figure 6 that the spectrum involves a six-line signal with $a^N = 13.1 \pm 0.1$ and $a^H_\beta = 7.9 \pm 0.3$ gauss that is similar to the signal obtained by computer simulation of a mixture of spin adducts of DMPO with alkoxy and aroyloxy radicals (see below). This six-line signal is not due to the adduct of DMPO with either NO or NO_2, since these adducts were found to give very different signals. (The NO and NO_2 spin adducts of DMPO give complex spectra of 7 and 15 lines, respectively.) The relative intensities of the signals obtained with DMPO do not change as a function of the smoking path length, in a manner similar to that observed for the PBN signals.

The effects of smoking path length on a^N and a^H_β values are also interesting. As can be seen in Table 5 and Figure 7, hfsc in the PBN system appear to be independent of the smoking path length. However, in the DMPO system, both a^N and a^H_β values show a slight variation with increasing path length, with a minimum value of the hfsc at about a 60 cm path length. These findings again indicate that at least two different types of signals, which have almost the same hfsc's in the PBN system, are present in the DMPO spin trap solution. Indeed, computer simulation shows that the change in the relative intensity of these two signals affects the value of a^N and a^H_β observed.

Effects of Aging and Radical Concentration

Measurements of the time dependence of the signals of the spin adducts also proved interesting. Figure 8 shows the results obtained 10 and 30 min after the initial measurement for the smoke-PBN system. Compared to Figure 5, it can

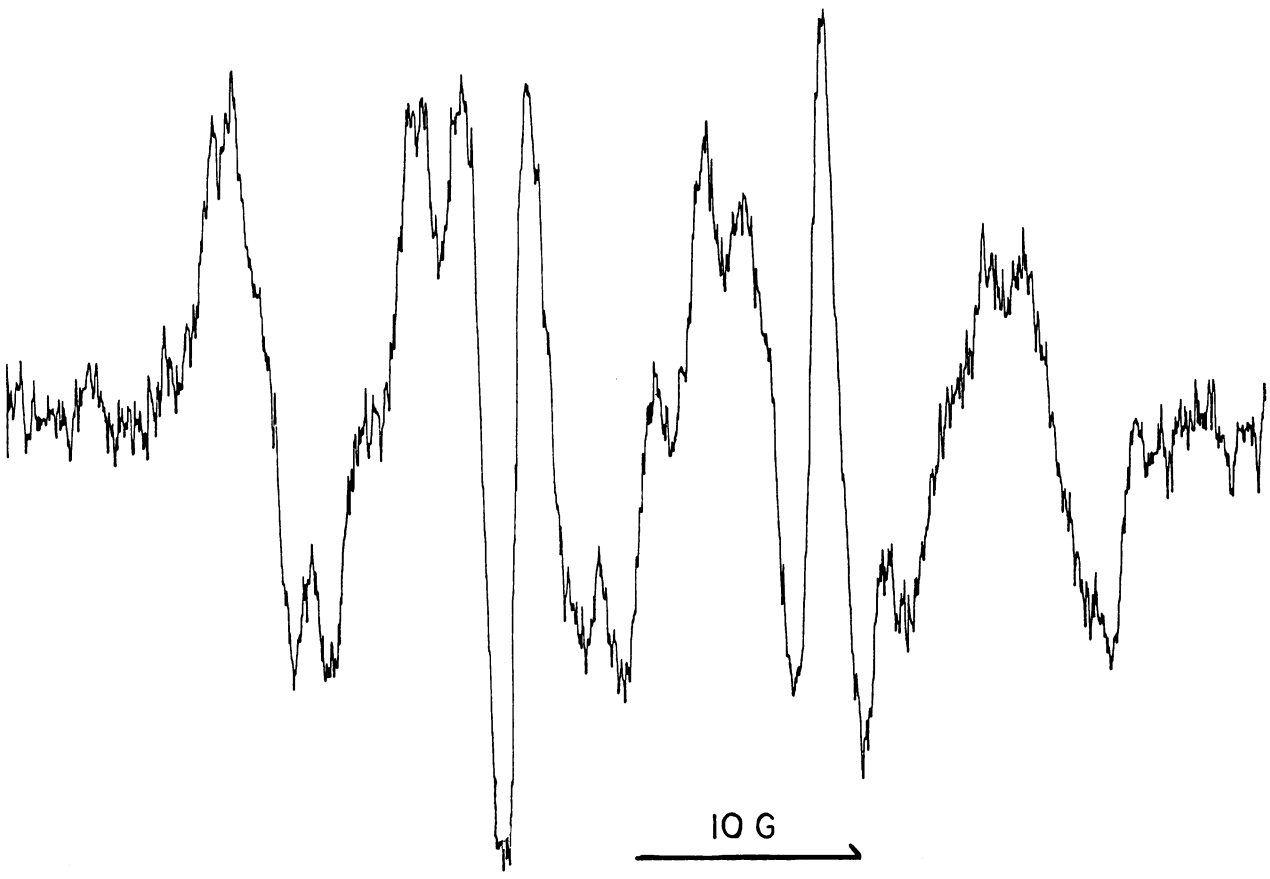

FIGURE 6. Typical ESR spectrum of smoke radicals-DMPO spin adducts in benzene obtained by using a 60 cm smoking path length.

be seen that the relative intensities of type I and II signals drastically change with time, suggesting that they arise from different types of radicals. The relative concentrations of radicals producing types I:II:III signals change from 110:20:1 in the initial measurement to 60:35:1 after 30 min. These changes correspond to a decrease in the relative area of the type I signal from 82% to 63%, and an increase in the relative size of the Type II signal from 17% to 36% of the total area. The relative area of type III radicals appears to remain constant at about 0.8% of the total area. Figure 9 graphically shows the results of the changes for the three types of smoke signals with time. The values given in Figure 9 were obtained by using a 60 cm smoking path length system.

It is obvious from Figure 9 that there is a great difference in the decay rate for the three types of signals. The ratio of decay rates is approximately 10^3:10^2:1 for type I:II:III signals during the initial 30 min.

de Hys and co-workers (*28*) report a significant change in the hfsc for the signals they observe from the smoke-PBN spin adduct upon aging the solutions. However, we do not find any change in the hfsc of the PBN spin adducts with time, despite the change in relative intensities described above.

The ESR spectrum of the smoke-DMPO spin adduct measured after aging for 40 min is shown in Figure 10. The spectrum in Figure 10 apparently consists of six lines with a^N = 13.7 and a_β^H= 11.3 gauss, values which are significantly different from the initial spectrum shown in Figure 6. It seems most reasonable to consider that this change results from the rapid decay of one component in the DMPO spin adduct solution.

The ESR spectra from a 60 cm path length experiment indicated a radical density of approximately 4×10^{14} spins/puff (or approximately 1×10^{16} spins/g of cigarette weight loss) assuming all smoke radicals are trapped by PBN. This value is close to those obtained by direct ESR measure-

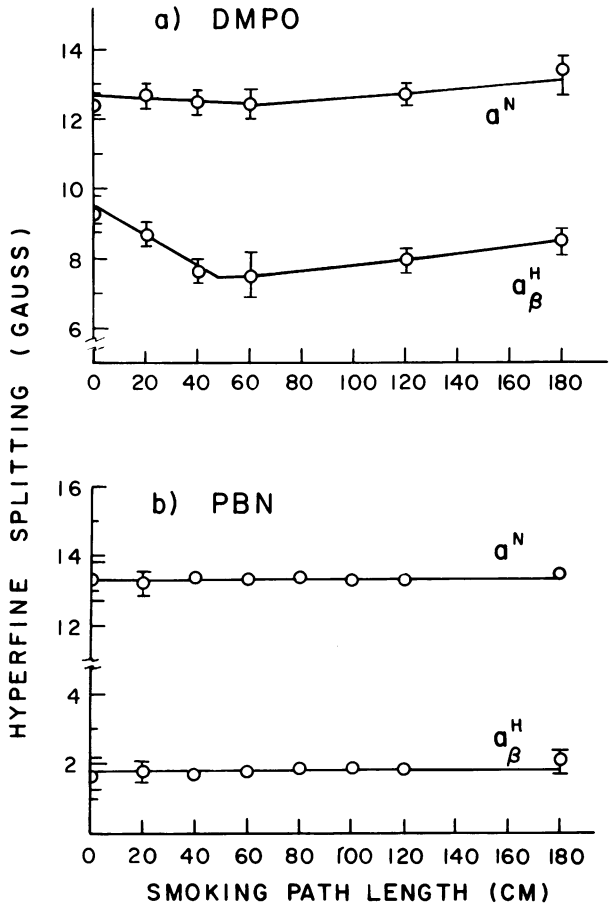

FIGURE 7. Effects of smoking path length on a^N and a^H_β values of (*a*) DMPO and (*b*) PBN spin adducts.

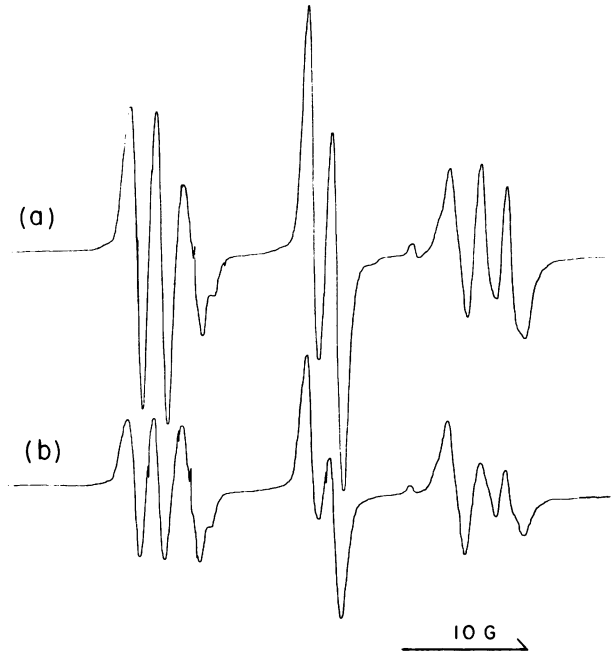

FIGURE 8. ESR spectral changes with time of cigarette smoke radicals-PBN spin adducts in a 60 cm path length system: (*a*) ca. 10 min and (*b*) 30 min after initial measurement.

ments on cigarette smoke condensate at 77°K (*8,16*). Menzel et al. (*33*) report the very much larger value of 10^{18} spins/puff of smoke using a technique based on line broadening of the smoke radical-PBN spin adduct at room temperature; their value would imply that 0.2% of the material in smoke contains an odd electron, a surprising result. For the 20 and 120 cm path lengths, we obtain 2 and 3×10^{14} spins/puff, respectively. These values show, as noted above, that higher concentrations of PBN spin adducts are obtained at intermediate path lengths. We have also duplicated Bluhm's experiment (*27*) using a Cambridge filter and find the concentration of radicals in smoke to be approximately 2.5×10^{14} spins/puff. Without a Cambridge filter we observe only a very weak signal.

To verify this effect of path length, the heights of the two central peaks in the ESR spectrum divided by gain are plotted versus the smoking path length in Figure 11. It is evident from Figure 11 that the condensed materials and smoke radical concentrations are a function of the smoking path lengths. Larger amounts of condensed materials were obtained in the shorter path length solution; for example, the amounts of condensed materials in 0, 60, and 120 cm path length systems were found to be 2.7, 1.1, and 0.6 mg, respectively (see Experimental Section).

Surprisingly however, the highest smoke radical concentrations were not obtained at the shortest path lengths (Fig. 11). Instead, the smoke radical concentration increases initially with path length to a maximum at 60 cm and then slowly decreases. We interpret this result as a competition between two opposing effects of changing path length: (1) radical concentration decreases as the path length is increased, which explains the decrease in ESR signal at long path lengths; (2) a high concentration of semivolatile particulate materials (PM) is aspirated and blown into the spin trap solutions at very short path lengths. Neurath (*34*) and Grob and Voellmin (*35*) have shown that a large number of organic compounds, including polynuclear aromatic hydrocarbons, phenols, aldehydes, and heterocyclic compounds, exist as "semivolatiles" (*36*) in tobacco smoke and can be volatilized again from a Cambridge filter after being trapped on it. These materials occur

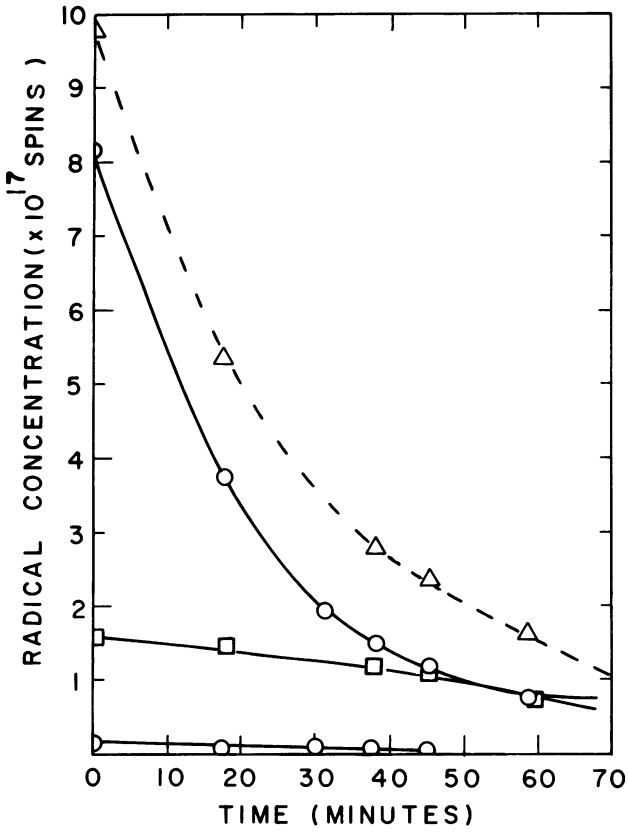

FIGURE 9. Time dependence of signal areas in cigarette smoke-PBN spin trapping system in benzene: (Δ) total, (O) type I, (□) type II, and (O, bottom) type III signal areas. These values were measured in a 60 cm smoking path length experiment.

in our system, and they probably react with radicals. In experiments at longer path length, most of these materials condense on the glass tubing of the smoking apparatus without reaching the trap solution, and therefore have little effect on the concentration of radicals observed. In the shorter path length experiments, more of these materials reach the spin trap solution and trap radicals, where they cause a decrease in the concentration of the spin-adduct radicals. In our present research, we are investigating two possible explanations of this phenomenon. One is that the materials in the particulate matter react with the spin adduct radicals as shown in eq. (3).

$$\text{Nitroxides of smoke radicals} + \text{PM} \longrightarrow \text{Products which do not give ESR signals} \quad (3)$$

In fact, our preliminary experiments do indicate that addition of PM in amounts comparable to that found in the smoke experiments results in a significant decay of $PhCO_2$- or *tert*-BuO-PBN spin adduct signals. We have also found that the initial rate of disappearance of these nitroxide radicals is first order in PM at room temperature.

The second possible interpretation of the path length effect is that condensed materials and PM compete with spin traps such as PBN to scavenge the smoke radicals and give products which do not exhibit ESR signals [eq.(4)].

Since the rate constants for trapping oxy radicals by PBN are 10^6-10^7 l./mole-sec (*25*), the condensed materials and particulate matter must

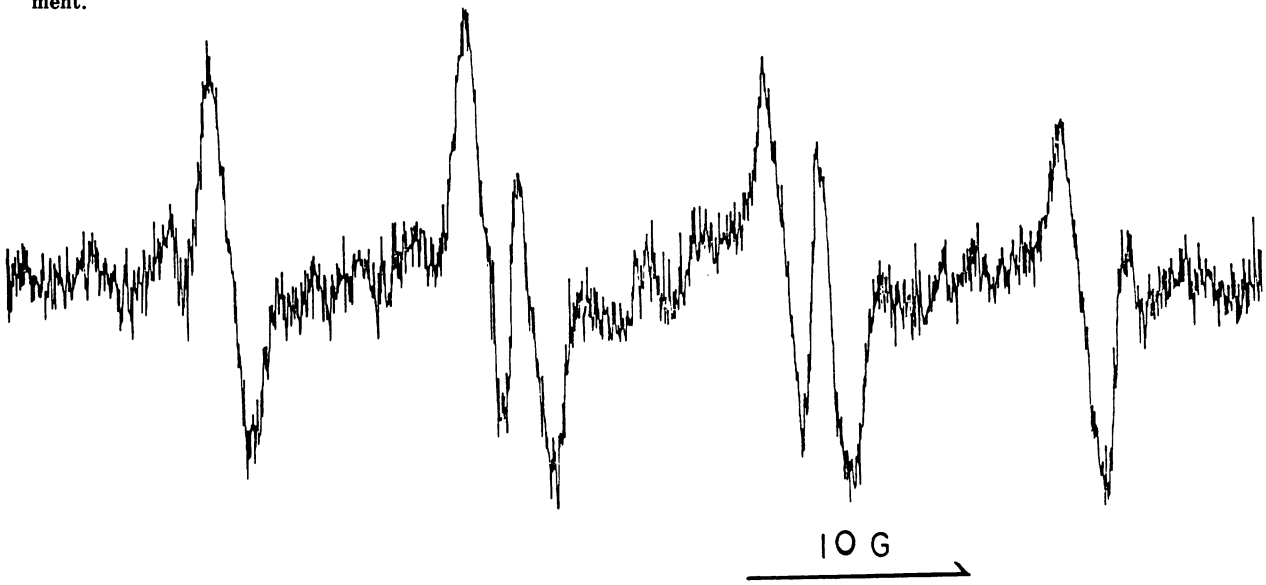

FIGURE 10. ESR spectral change in smoke radicals-DMPO spin adduct of a 60 cm path length system in benzene measured 40 min after the initial measurement which is shown in Fig. 6.

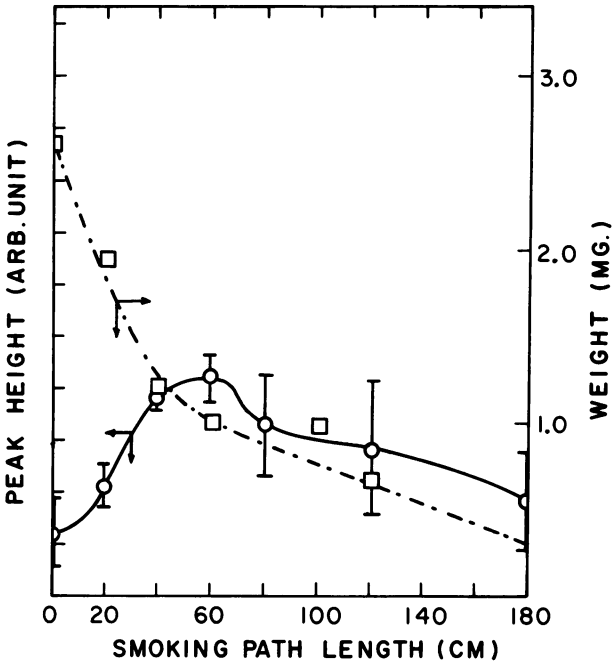

FIGURE 11. Dependence of the relative intensity of smoke radicals-PBN spin adducts signals and weight of condensed materials on the smoking path lengths; vertical lines indicate standard errors.

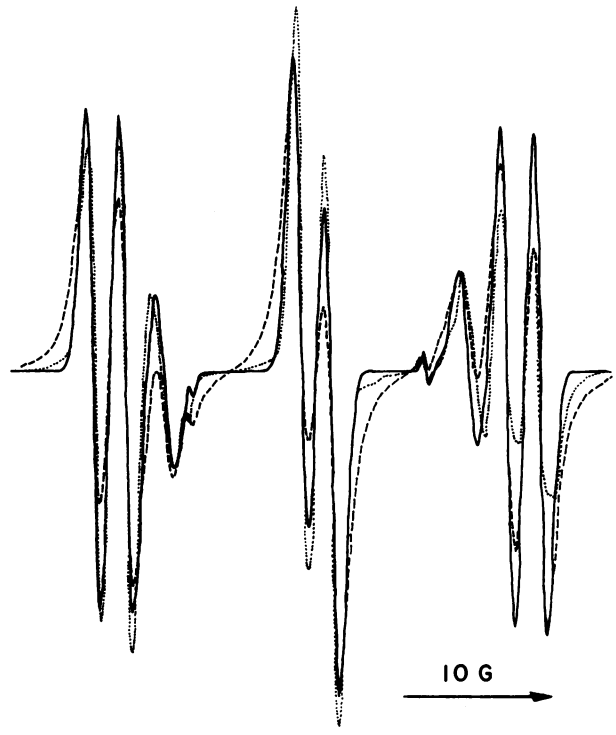

FIGURE 12. Simulated ESR spectra of the *t*-BuO- and $PhCO_2$-PBN, type II, and type III signals for the 60 cm path length system: (——), Gaussian; (---), Lorentzian; (· · ·), observed spectrum from eight cigarettes. Parameters for *t*-BuO-PBN, $PhCO_2$-PBN, type II, and type III: relative intensity: 0.9:0.1:0.4:0.0035; *g* values: 2.0061, 2.0061, 2.0061, 2.0064; line width: 0.950, 0.780, 1.525, 0.440 gauss, respectively.

$$\text{Smoke radicals} + \text{PM} \longrightarrow \text{Products which do not give ESR signals} \quad (4a)$$

$$\text{Smoke radicals} + \text{PBN} \longrightarrow \text{Spin adduct} \quad (4b)$$

react with smoke radicals very rapidly. This is not unexpected; we will refer to this possibility later.

Computer Simulation

To further elucidate the spectra obtained in this study, computer simulation was employed. The simulated ESR spectra obtained by use of our data on PBN spin adducts of benzoyloxy ($PhCO_2\cdot$) and *tert*-butoxy (*t*-BuO·) radicals (Table 1) and the data on type II and III signals are illustrated in Figure 12, in which the solid and dashed curves represent the data obtained for Gaussian and Lorentzian line shapes, respectively. As is obvious from Figure 12, the Gaussian curve appears to coincide best with the observed spectrum (the dotted line) in the system with 60 cm smoking path length. The agreement between the simulated and observed spectra strongly suggests that the ESR signals observed as a set of three doublets (type I) may involve two different kinds of nitroxides such as $PhCO_2\cdot$ and *t*-BuO· spin adducts; this will be discussed later. The spectra obtained from shorter path lengths could be also simulated by using slightly larger line widths for the PBN spin adduct, suggestive of line broadening. These computed spectra are depicted in Figure 13. The observed spectrum in the smoke system appears to fit a Lorentzian curve best, as can be seen in Figure 13.

Similarly, a simulation of the spectra of smoke radical-DMPO spin adducts (Figs. 4 and 6) was performed. Figure 4 shows a broad six-line spectrum without any of the γ-hydrogen splitting that is observed in the longer path length spectrum (Fig. 6). Although this difference in γ-hydrogen splitting could indicate different radicals in these two spectra, we believe that line broadening in Figure 4 hides these splittings which are superimposed on the narrower lines in Figure 6. The simulated spectra of Figure 4 using our data for DMPO spin adducts of PhCO· and *t*-BuO· radicals (Table I) are illustrated in Figure 14, in which the simulated Gaussian and Lorentzian lines are

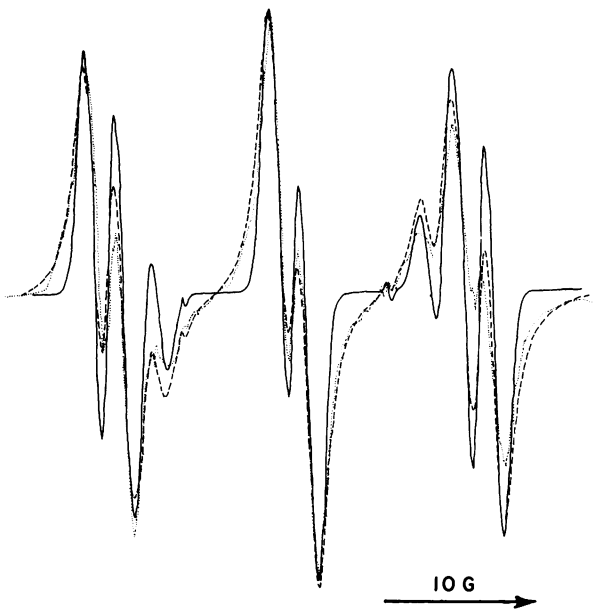

FIGURE 13. Simulated ESR spectra of the *t*-BuO- and $PhCO_2$-PBN, type II, and type III signals for the short path length system: (———) Gaussian; (---) Lorentzian; (. . .) observed spectrum from nine cigarettes. Parameters used for *t*-BuO-PBN, $PhCO_2$-PBN, type II, and type III; relative intensity: 0.9:0.1:0.20:0.0015; *g* values: 2.0061, 2.0061, 2.0061, 2.0061, 2.0064; line width: 1.229, 0.850, 1.525, 0..440 gauss, respectively.

given as solid and dashed lines, respectively, while the dotted line represents the observed spectrum. The simulated spectra of Figure 6 are likewise given in Figure 15. The simulated spectra do not fit the observed spectra very well; therefore, although the hfsc values obtained from the simulations ($a^N \cong 12.6$ and $a^H_\beta \cong 7.1$ gauss) are suggestive of the values for spin adducts of $PhCO_2\cdot$ and *t*-BuO· radicals, the poor fit could indicate the presence of other radicals in this system.

These computer simulations also emphasize the line broadening which occurs in the shorter path length experiments. Because of this path length dependence, we believe that this broadening results from interaction of the spin adduct radicals with PM in the spin trapping solution. Line broadening due to a decrease in spin-lattice relaxation time (radical lifetime) is relatively unimportant for these stable nitroxide radicals; rather a decrease in the spin-spin relaxation time caused perhaps by electron-spin exchange or dipolar interactions probably produces this linewidth effect.

Discussion

The formation of typical nitroxide spin adducts with observable β-hydrogen hfsc from cigarette smoke was observed using both PBN and DMPO. The long path length experiments with PBN are perhaps the most revealing. We interpret the ESR spectra observed in this system (see Fig. 5) as being composed of three types of signals. Signals of types II and III we tentatively assign to one-electron oxidation products of PBN. The hfsc for the type I signal (Table 5) are $a^N \cong 13.8$ and $a^H_\beta \cong 1.9$ gauss. These values appear to be a combination of the hfsc values for the *tert*-butoxy and benzoyloxy spin adducts (see Table 1). The presence of alkoxy radicals in smoke also has been suggested by Bluhm et al. (*27*), who report the formation of a PBN spin adduct with $a^N = 13.7$ and $a^H_\beta = 1.99$ gauss.

The spectral changes obtained from the time dependence of the DMPO signals indicate the existence of several types of radicals in this system also. The ESR spectrum (Fig. 10) with $a^N = 13.7$ and $a^H_\beta = 11.3$ gauss, which was obtained about 40 min after the initial spectrum shown in Figure 6, also appears to have characteristics of both alkoxy and aroyloxy radicals (compare Tables 1 and 5).

Therefore, we suggest that type I signals result from spin adducts of both alkoxy and aroyloxy radicals. Although the individual hfsc in Table 1 do not agree exactly with those for type I radicals, computer simulations of the spectra which result from a mixture of spin adducts from both alkoxy and aroyloxy radicals with PBN and DMPO agree satisfactorily with the observed spectra (see Figs.12-15.)

Our present data do not allow us to specify the nature of either the aromatic group in $ArCO_2\cdot$ or the alkyl group in the RO· radicals. However, since the path lengths in these experiments are relatively long, and since tertiary alkoxy radicals are longer-lived than primary or secondary (*37*), it is not unreasonable to suggest that the alkoxy radicals are mainly tertiary with structures like that of the *tert*-butoxy radical we have used as a model.

The absence of carbon-centered radicals is indicated by the data from both the PBN and the DMPO systems. This is confirmed by studies using OHPBN, a spin trap that gives different kinds of signals for oxygen- and carbon-centered radicals. It is not surprising that carbon-centered radicals are not observed as spin adducts in our system, since they would be expected to react rapidly with oxygen before they reach the spin trap solution. The basis of this expectation is the following. The rate constant for the reaction of simple alkyl radicals with oxygen is very fast, approximately 10^9 l./mole-sec (*37*). Johnson et al.

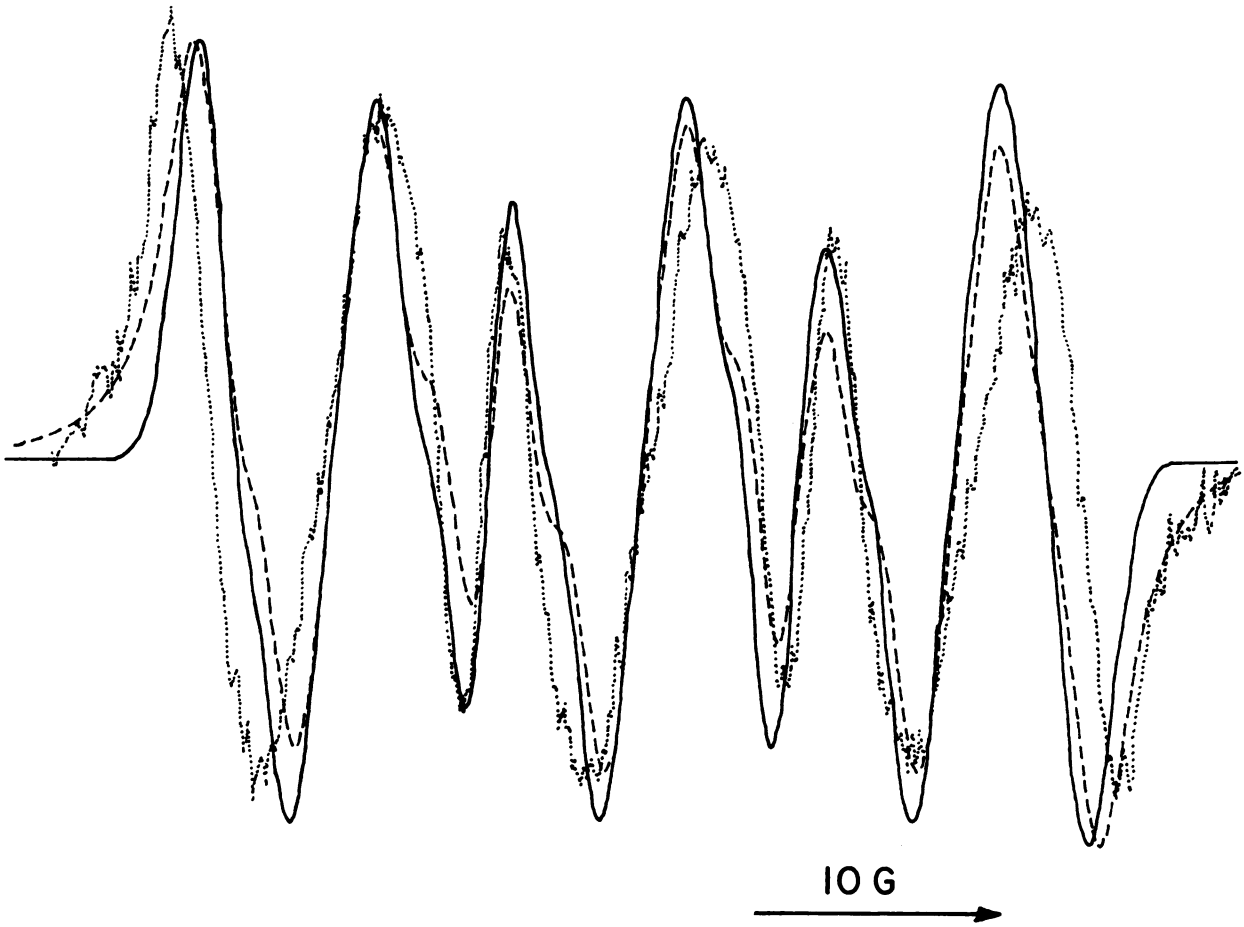

FIGURE 14. Simulated ESR spectra of the *t*-BuO- and $PhCO_2$-DMPO system: (——) Gaussian; (---) Lorentzian, (· · ·) Observed spectrum from eight cigarettes in the short path length (0 cm) system. Parameters used for *t*-BuO-DMPO and $PhCO_2$-DMPO: relative intensity: 0.95:0.05; *g* values: 2.00652, 2.00674; line width: 2.34, 1.72 gauss, respectively.

(*38*), using $^{18}O_2$-labeled air, demonstrated that appreciable oxygenation of the material in smoke occurs. Thus, although carbon radicals undoubtedly are present, they are converted to oxygenated radicals before they can be trapped.

It might appear surprising that only alkoxy radicals and not peroxy radicals are trapped. However, studies of the autoxidation of hydrocarbons indicate that the peroxy radicals initially formed can react to produce alkoxy radicals. For example, they can dimerize to form two alkoxy radicals and a molecule of oxygen (*37*). They also can abstract hydrogen to produce unstable hydroperoxides, ROOH (*39-42*). The homolysis of these hydroperoxides can be assisted by olefins, aldehydes and ketones, carboxylic acids, alcohols, amines and amine salts, or other molecules of hydroperoxide; in other words, by practically any organic compound (*43*). Moreover, tobacco contains various metallic compounds involving iron, maganese, copper, zinc, and nickel (*3*), traces of which are known to induce the homolytic decomposition of hydroperoxides at room temperature (*43*). In addition, peroxy radicals are converted to alkoxy radicals by reaction with a number of reagents (olefins, amines, sulfides) in oxygen-transfer reactions.

The production of aroyloxy-type radicals could result from the oxidation of aldehydes. Extensive analyses of tobacco constituents have shown the presence of both aromatic aldehydes (*44*) and considerable amounts (*45*) of carbonyl constituents (16-34 mg/100 g dry weight). In addition, the acidic constituents are more than 20% of the dry leaf weight (*46*).

We suggest the two possible mechanisms to explain the path length effect observed in this study. One is related to the stability of nitroxide radicals [eq. (3)]. The other mechanism, shown in eq. (4a), is related to the reactivity of the smoke

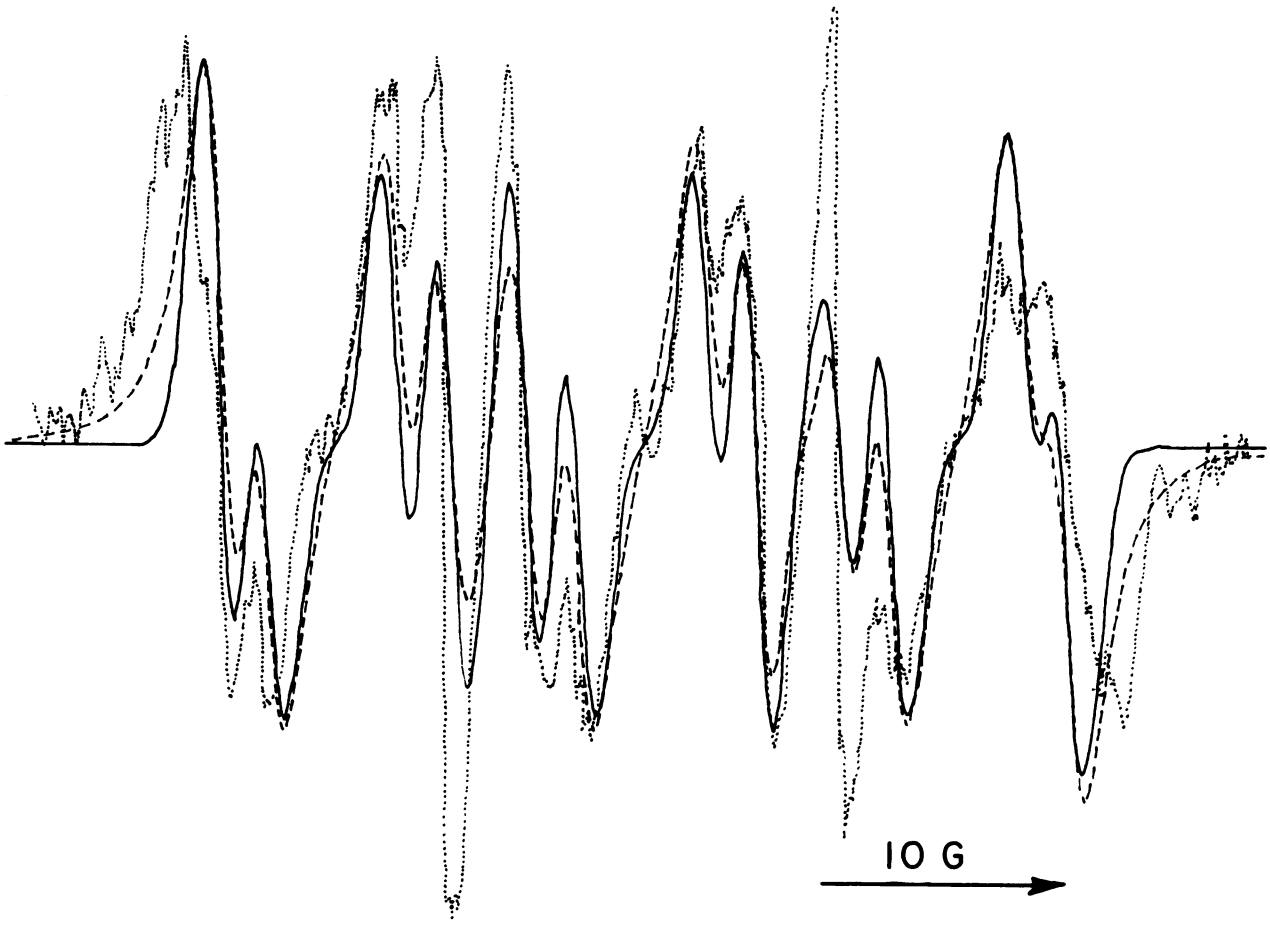

FIGURE 15. Simulated ESR spectra of the *t*-BuO- and $PhCO_2$-DMPO system: (——), Gaussian; (---), Lorentzian; (· · ·), observed spectrum from eight cigarettes in the 60 cm path length system. Parameters used for *t*-BuO-DMPO and $PhCO_2$-DMPO; relative intensity: 0.80:0.20; *g* values: 2.00652, 2.00674; line width: 1.60, 1.72 gauss, respectively.

radicals and might have important implications on the carcinogenicity of cigarette smoke. We suggest that smoke radicals may be able to convert aromatic compounds to arene oxide or hydroxide.

$$ArH \xrightarrow[\text{smoke}]{\text{Radicals in}} \text{Arene oxide} \longrightarrow ArOH \qquad (5)$$

derivatives [eq. (5)]. It is known that aromatic hydrocarbons themselves are not carcinogenic but that their oxides and hydroxy derivatives may be (*47-53*). It also is known (*54, 55*) that peroxy radicals convert olefins to epoxides [eq. (6)]. Thus we suggest that aromatic hydrocarbons

$$ROO\cdot + R_2C{=}CR_2 \longrightarrow RO\cdot + R_2C\overset{O}{\diagup\diagdown}CR_2 \qquad (6)$$

in smoke might react with peroxy radicals in smoke to produce arene epoxides; these are known to be converted to aromatic hydroxy derivatives (*56-59*). Thus, smoke may contain both precarcinogens and the reactive species capable of converting them to active carcinogens.

The authors thank Professor Brian Hales for helpful discussions and Mr. L. S. Edelen for skillful technical assistance. This research was supported by the National Institutes of Health, Grant HL-16029.

REFERENCES

1. U.S. Public Health Service, The Health Consequences of Smoking. A Report of the Surgeon General: U.S. Department of Health, Education and Welfare Washington, D.C., 1972.
2. Schmeltz, I., Ed., The Chemistry of Tobacco and Tobacco Smoke, Plenum Press, New York, 1972, pp. 12, 65-105.
3. Wynder, E. L., and Hoffmann, D. Studies in experimental carcinogenesis. In: Tobacco and Tobacco Smoke, Academic Press, New York, 1967, Chapts. 7 and 8.

4. Pryor, W. A. Free radicals in biological systems. Sci. American 223: No. 2, 70 (Aug. 1970).
5. Passwater, R. A. Cancer: new direction. Am. Lab. (June 1973).
6. Swartz, H. M. Electron spin resonance studies of carcinogenesis. Advan. Cancer Res. 15: 227 (1972).
7. Rowlands, J. R., and Gause, E. M. Spectroscopic investigation of effects of tobacco smoke constituents on mammals. Final Report for the Council for Tobacco Research (U.S.), Proj. No. 05-2975-01, 1971.
8. Buell, G. C. Biochemical parameters in inhalation carcinogenesis. In: Inhalation Carcinogenesis, M. G. Hanna, Jr., P. Nettesheim, and J. R. Gilbert, Eds., U.S. Atomic Energy Commission, National Bureau of Standards, CONF-691001, Springfield, Va. 1970, pp 209-228.
9. Rowlands, J. R., et al. An electron spin resonance study of tobacco smoke condensates and their effects upon blood constituents. Environ. Res., 2:47 (1968).
10. Green, G. M., and Carolin, D. The depressant effect of cigarette smoke on the *in vitro* antibacterial activity of alveolar macrophages. New Engl. J. Med. 276: 421 (1967).
11. Green, G. M. Cigarette smoke: protection of alveolar macrophages by glutathione and cysteine. Science 162: 810 (1968).
12. Lyons, M. J., Gibson, J. K., and Ingram, D. J. E. Free-radicals produced in cigarette smoke. Nature 181: 1003 (1958).
13. Tully, G. W., and Briggs, C. D. E. P. R. absorption by the vapour phase of cigarette smoke, condensed and examined at low temperature. Chem. Ind., (London) 1969: 201.
14. Forbes, W. F., Robinson, J. C., and Wright, G. F. Free radicals of biological interest. Can. J. Biochem., 45: 1087 (1967).
15. Rowlands, J. R., Cadens, D. G., Jr., and Gross, A. L. Effects of tobacco smoke on lung tissue as measured by electron spin resonance. Nature 213: 1256 (1967).
16. Ingram, D. J. E. Electron resonance studies of the free radicals produced in tobacco pyrolysis and in other related compounds. Acta Med. Scand, (Suppl.), 369: 43 (1961).
17. Cooper, J. T., Forbes, W. F., and Robinson, J. C. (1971). Free radicals as possible contributors to tobacco-smoke carcinogenesis. National Cancer Inst. Monograph No. 28, NCI, Washington, D. C. 1971, pp. 191-197.
18. Leuchtenberger, C., and Leuchtenberger, R. Effects of chronic inhalation of whole fresh cigarette smoke and of its gas phase on pulmonary tumorigenesis in Snell's mice. In: Morphology of Experimental Respiratory Carcinogenesis, P. Nettesheim, M. G. Hanna, Jr., and J. W. Deatherage, Jr., Eds., U. S. Atomic Energy Commission, CONF-700501, National Technical Information Service, Department of Commerce, Springfield, Va. 1970, pp. 329-346.
19. Janzen, E. G. Spin trapping. Accts. Chem. Res., 4: 31 (1971), and references therein.
20. Lagercrantz, C. Spin trapping of some short-lived radicals by the nitroxide method. J. Phys. Chem. 75: 3466 (1971), and references therein.
21. Perkins, M. J. The trapping of free radicals by diamagnetic scavengers. Special Pub. No. 24, Chem. Soc., London, 1970, pp. 97-115.
22. Bonnet, R., et al. Experiments toward the synthesis of corrins. Part II. The preparation and reactions of Δ^1-pyrroline oxides. J. Chem. Soc. 1959: 2094.
23. Emmons, W. D. The preparation and properties of oxaziranes. J. Amer. Chem. Soc. 79: 5739 (1957).
24. Bluhm, A. L., and Weinstein, J. α-Phenylnitroxide radicals from α-phenylnitrones. J. Org. Chem. 37: 1748 (1972).
25. Janzen, E. G., and Evans, C. A. Rate constants for the addition of phenyl radicals to PBN and benzene as studied by ESR. J. Amer. Chem. Soc. 97: 205 (1975).
26. Janzen, E. G., and Blackburn, B. J. Detection and identification of short-lived free radicals by electron spin resonance trapping techniques. J. Amer. Chem. Soc., 91: 4481 (1969).
27. Bluhm, A. L., Weinstein, J., and Sousa, J. A. Free radicals in tobacco smoke. Nature 229: 500 (1971).
28. de Hys, L. S., et al. Electron spin resonance spin trapping studies of cigarette smoke. Proc. Tobacco Health Workshop Conf., 4th Conf., 1973, pp. 474-483.
29. Janzen, E. G., and Liu, J. I. P. Spin trapping. J. Magnetic Res., 9: 510 (1973).
30. Pacifici, J. G., and Browning, H. L., Jr. A novel probe for radical detection and identification. J. Amer. Chem. Soc., 92: 5231 (1970).
31. Bokhoven, C., and Niessen, H. J. Amounts of oxides of nitrogen and carbon monoxide in cigarette smoke, with and without inhalation. Nature 192: 458-459 (1951).
32. Norman, V., and Keith, C. H. Nitrogen oxides in tobacco smoke. Nature 205: 915 (1965).
33. Menzel, E. R., Vincent, W. R., and Wasson, J. R. Dipolar broadening of electron spin resonance lines of free radicals—Spin trapping studies of free radicals in cigarette smoke. J. Magnetic Res., in press.
34. Neurath, G. B. Recent advances in knowledge of the chemical composition of tobacco smoke. In: The Chemistry of Tobacco and Tobacco Smoke, I. Schmeltz, Ed., Plenum Press, New York, 1972, pp. 77-97.
35. Grob, K., and Voellmin, J. A. GC-MS analysis of the "semi-volatiles" of cigarette smoke. J. Chromatog. Sci., 8: 218 (1970).
36. Williamson, J. T., Graham, J. F., and Allman, D. R. Beit. Tabakforsch. 3: 233. 1965; cited in: The Chemistry of Tobacco and Tobacco Smoke, I. Schmeltz, Ed., Plenum Press, New York, 1972, pp. 77-105.
37. Howard, J. A. Homogeneous liquid-phase autoxidations. In: Free Radicals, J. K. Kochi, Ed., Vol. II John Wiley and Sons, New York, Chapt. 12.
38. Johnson, W. R., et al. Incorporation of atmospheric oxygen into components of cigarette smoke. Chem. Ind. (London) 1975: 521.
39. Walling, C., and Heaton, L. Radical formation in the reactions of *t*-butyl hydroperoxide with styrene. J. Amer. Chem. Soc., 87: 38 (1965).
40. Pryor, W. A. Free Radicals, McGraw-Hill, New York, 1966, pp. 113-126.
41. Hiatt, R., and Irwin, K. C. Homolytic decompositions of hydroperoxides. V. Thermal decompositions. J. Org. Chem. 33: 1436 (1967).
42. Kirk, A. D. The thermal decomposition of methyl hydroperoxide. Can. J. Chem., 43: 2236 (1965).
43. Hiatt, R. Hydroperoxides. In: Organic Peroxides, D. Swern, Ed., Wiley-Interscience, New York, 1971 Chap. 1.
44. Yang, C. H., and Wender, S. H. Identification of aromatic aldehydes in cigarette smoke and in tobacco. Phytochemistry 3: 17(1964).
45. Weybrew, J. A., and Stephenos, R. L. Survey of the carbonyl contents of tobacco. Tobacco Sci. 6, 53 (1962).
46. Schlotzhauer, W. S., Higman, E. B., and Schmeltz, I. Pyrolysis of tobacco extracts. In: The Chemistry of Tobacco and Tobacco Smoke, I. Schmeltz, Ed., Plenum Press, New York, 1972, pp. 65-76.
47. Welch, R. M., Loh, A., and Conney, A. H. Cigarette Smoke: stimulatory effect on metabolism of 3,4-benzpyrene by enzymes in rat lung. Life Sci. 10, 215 (1971).

48. Alexandrov, K., and Frayssinet, C. The effect of cigarette-smoke condensate on the in vitro fixation of benzo[a]pyrene on DNA. Experientia 28: 932 (1972).
49. Marquardt, H., et al. Malignant transformation of cells derived from mouse prostate by epoxides and other derivatives of polycyclic hydrocarbons. Cancer Res. 32: 716 (1972).
50. Huberman, E., et al. Transformation of hamster embryo cells by epoxides and other derivatives of polycyclic hydrocarbons. Cancer Res. 32: 1391 (1972).
51. Gelboin, H. V. Kinoshita, N., and Wiebel, F. J. Microsomal hydroxylases: induction and role in polycyclic hydrocarbon carcinogenesis and toxicity. Fed. Proc., 31: 1298 (1972).
52. Fahmy, O. G., and Fahmy, M. J. Oxidative activation of benz[a]-anthracene and methylated derivatives in mutagenesis and carcinogenesis. Cancer Res. 33: 2354 (1973).
53. Jerina, D. M., and Daly, J. W. Arene oxides: a new aspect a drug metabolism, Science 185: 573 (1974).
54. Mayo, F. R. The oxidation of unsaturated compounds. V. The effect of oxygen pressure on the oxidation of styrene. J. Amer. Chem. Soc. 80: 2465 (1958).
55. Mayo, F. R. Free radical autoxidation of hydrocarbons. Accts. Chem. Res. 1: 193 (1968).
56. Jerina, D., et al. Role of the arene oxide-oxepin system in the metabolism of aromatic substrates. I. *In vitro* conversion of benzene oxide to a permercapturic acid and a dihydrodiol. Arch. Biochem. Biophys. 128: 176 (1968).
57. Jerina, D. M., et al. 1,2-Naphthalene oxide as an intermediate in the microsomal hydroxylation of naphthalene. Biochemistry, 9: 147 (1970).
58. DeMarinis, R. M., and Berchtold, G. A. Reaction of oxepine-benzene oxide with nucleophiles. J. Amer. Chem. Soc. 91: 6525 (1969).
59. Daly, J. W., Jerina, D. M., and Witkop, B. Arene oxides and the NIH shift: The metabolism, toxicity and carcinogenicity of aromatic compounds. Experientia 28: 1129 (1972).